SMART CEMENT COMPOSITES CHARACTERIZATION AND CORROSION DETECTION AND QUANTIFICATION USING REAL-TIME MONITORING SYSTEMS: DEVELOPMENTS AND MODELING

C. Vipulanandan Ph.D., P.E.

Center for Innovative Grouting Material and Technology (CIGMAT)
Department of Civil and Environmental Engineering
University of Houston, Houston, Texas 77204-4003

Abstract

Smart cement composites with highly sensing chemo-thermo-piezoresistive properties with enhanced physical and mechanical properties have been developed and characterized to meet the various application requirements with real-time monitoring. In this study, smart cement was modified with foam, iron nano particles and aggregates. Smart cement (class H oil well cement) with water-to-cement ratio of 0.38 was modified with 5% and 20% (by weight). The density of the smart cement was 16.3 ppg and with 20% foam it reduced to 9 ppg, a 45% reduction. Addition of 20% foam, reduced the thermal conductivity of the smart cement by 65%. The smart cement slurries with and without foam were piezoresistive. The resistivity change at 4 MPa (600 psi) increased from 8% for the smart cement slurry with no foam to 22% with 20% foam, about 175% increase in the piezoresistivity. The total fluid loss for the smart cement at 0.7 MPa (100 psi) pressure was reduced from 134 mL to 13 mL with the addition of 20% foam, about a 90% reduction. The electrical resistivity changes of the hydrating cement was influenced by the amount of foam in the cement. Addition of 20% foam increased the initial electrical resistivity of smart cement from 1.05 Ωm to 2.04 Ωm, a 94% increase. The one day compressive strength of smart cement was reduced to 0.57 MPa (220 psi) from 10.3 MPa (1500 psi) with the addition of 20% foam, a 83% reduction. The solidified smart cement with and without foam were piezoresistive.

Addition of 1% NanoFe_2O_3 increased the compressive strength of the smart cement by 26% and 40% after 1 day and 28 days of curing respectively. The modulus of elasticity of the smart cement increased with the additional of 1% NanoFe_2O_3 by 29% and 28% after 1 day and 28 days of curing respectively. Addition of 1% nanoFe2O3 also enhanced the piezoresistivity behaviour of the smart cement. With the addition of 10%, 50% and 75% of gravel (by weight of the total mix) to the smart cement, the piezoresistivity at peak compressive stress decreased by 6%, 23% and 42% respectively after one day of curing. The corrosion of steel was direction and with current monitoring approach the bulk and surface corrosion of the steel was quantified in terms of electrical resistivity and a new interface coupling parameter respectively. The directional resistivity changes during corrosion were much higher than the weight change and the pulse velocity change.

The Vipulanandan p-q curing, stress-strain and piezoresistive models predicated the experimental results very well. Also the Vipulanandan Impedance-frequency model predicted both the smart cement composites and steel corrosion behaviors.

1. Introduction

Cement is the largest quantity of material manufactured in the world and used in many applications. Also the cements are produced with varying chemical composition and are classified in the various classes. Cements are used as grout and coatings (water-cement mix), mortar (water-cement-sand mix) and concrete (water-cement-aggregates mix). Environmental and economic concerns with some of the reported cementing failures in the oil and gas industry have demanded for the development of new innovative technologies for real-time monitoring of the wells. Oil well cement serves many purposes in the cemented oil and gas wells. Foremost important among these is to form a sealing layer between the well casing and the geological formation referred to as the zone of isolation. Past four decades of offshore well failures in the offshore of U.S. have clearly identified cementing failures as the major cause for blowouts (Izon et al. 2007). Also the deep-water horizon blowout in 2010 in the Gulf of Mexico was due to cementing issues (Carter et al. 2014; Kyle et al. 2014). Therefore, real-time monitoring and tracking the process of well cementing and the performance during the entire service life has become important to ensure cement integrity (Vipulanandan et al. 2014 (a)-(d); Zhang et al. 2010 (a)-(b)).

Smart Cement

Smart cement has been developed (Vipulanandan et al. 2014-2016) which can sense many changes happening inside the borehole during cementing to curing after the concreting jobs. The smart cement can sense the changes in the water-to-cement ratios, different additives, and any pressure applied to the cement sheath in terms of chemo-thermo-piezoresistivity. The failure compressive strain for the smart cement was 0.2% at peak compressive stress and the resistivity change is of the order of several hundred pecentage making it over 500 times more sensitive (Vipulanandan et al. 2014-2016).

Foam

Foam addition to cement provides particular benefits in to deepwater wells due to its lower thermal conductivity and enhanced flexibility. A low thermal conductivity cement sheath allows for less and slower heat transfer/heat loss in the wellbore. This benefit will allow for more productive steam-generating wells in geothermal projects. These enhanced mechanical properties will allow more flexibility for the cement sheath to respond to the effects of excessive temperatures in the wellbore, therefore maintaining cement sheath integrity and providing zonal isolation/casing protection. Enhanced and highly-engineered mechanical properties of the foam cement sheath allow it to move with the wellbore and also absorb stresses resulting from the mechanical shocks from pipe tripping to expansion and contraction of the casing during pressure and well testing, thermal shocks and during the injection and production cycling.

Importantly, foam cement is expected to establish a tight bond for a reliable annular seal because the nitrogen bubbles help to prevent shrinkage while the cement slurry goes through the hydration stage. A foamed system, due to its expansion properties, also accommodates challenging wellbore geometries such as wash-outs. It is important to note that foam cement has historically been used primarily for reduction of slurry density. Also foam cement systems much lighter than water, yet without compromising essential mechanical properties to establish life-of-the-well zonal isolation

has been reported in the literature.

Iron Nanomaterials

With the advancement of nanotechnology, polymer science and engineering, several of these materials can be a key to solving some of the problems encountered in oil and gas well cementing. One of which is the use of nanotechnology and hence, nanomaterials which are beneficial for their large surface area, high aspect ratio, small size, low density and interesting physical and chemical properties. Several reasons nanoparticles have had such a strong influence on the mechanical properties of cementitious materials become the nanoparticles have a high surface area, providing high chemical reactivity. Also owing to the fact that the C−S−H gel diameter is approximately 10 nm, the dispersed nanoparticles can fill the voids between cement grains, resulting in denser material. Well-dispersed nanoparticles act as reaction centers, accelerating cement hydration because of the high reactivity of nanoparticles. Also highly reactive nanoparticles accelerate the pozzolanic reaction and also react with $Ca(OH)_2$. Nanoparticles have been also added to drilling muds in small amounts, with amounts of the order of 1% to enhance the performance based on the environmental conditions. Nanotechnologies are also being developed to enable and enhance down-hole sensors and actuators that can operate in chemically harsh environmental at high pressures and temperatures.

Aggregates

Aggregates of various types and grades are used in making cement mortar and concrete. Aggregates are used to enhance the physical and mechanical properties of the cement mortar and concrete in addition make it a very cost effective construction material.

Corrosion

Around the world, one of the foremost long term durability problem encountered is corrosion and estimated losses are over billions of dollars per year. Corrosion is the destructive attack on a material by bio-physio-chemical reactions with the exposed environment. In addition to our everyday encounters with this kind of degradation, corrosion causes plant shutdowns, waste of valuable resources, loss or contamination of product, reduction in potency, expensive maintenance, and costly over-design, it additionally jeopardizes the safety and inhibits technological progress. .

2. Objective

The overall objective of this work was to not only develop smart cement composites for various applications but also detect and quantify corrosion with real-time monitoring systems.

The specific objectives were as follows:

(1) Develop and characterize smart cement composites with foam, iron nanoparticles and aggregates.

(2) Detect and quantify in anisotropic and heterogeneous corrosion (directional) in

steel by developing new concepts for real-time monitoring.

(3) Model the observed smart cement composites and corrosion behaviors for use in real-time monitoring.

3. Theory and Concept

Vipulanandan Impedance Model (Vipulanandan et al., 2013)
Equivalent Circuit.

It is important to identify the most appropriate equivalent circuit to represent the electrical properties of uncorroded and corroded materials to characterize its performace with time. In this study, two different possible equivalent circuits were analyzed to find an appropriate equivalent circuit to represent smart cement composites and corroded steel.

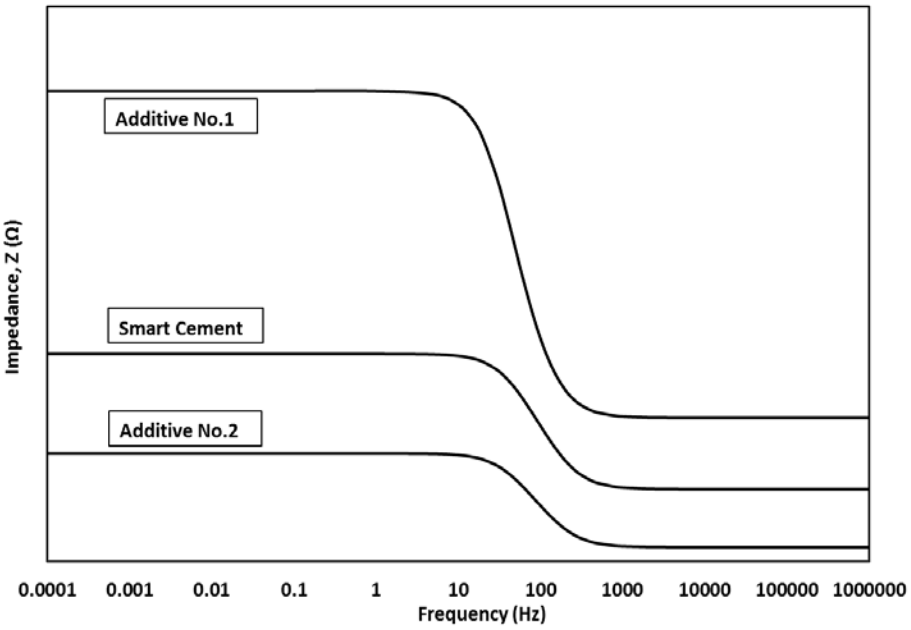

Figure 1. Impedance- frequancy (A.C.) Relationshipe for Smart Cement With Additives and Corroding Steel

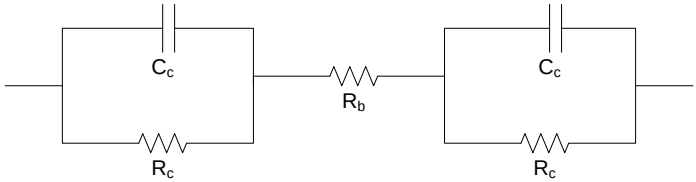

Figure 2. Equivalent Circuit for Case 2

Based on the two probe measurement the impedance–frequency relationship was Case 2 which represents a resistive bulk material and the impedance of the equivalent circuit for Case 2 (Z_2) is as follows (Vipulanandan Impedance – Frequency Model):

$$Z_2(\sigma) = R_b(\sigma) + \frac{2R_c(\sigma)}{1+\omega^2 R_c^2 C_c^2} - j\frac{2\omega R_c^2 C_c(\sigma)}{1+\omega^2 R_c^2 C_c^2}. \quad (1)$$

When the frequency (f) of the applied signal is very low, ω (= $2\pi f$) $\rightarrow$ 0, $Z_2 = R_b + 2R_c$, and when it is very high, $\omega \rightarrow \infty$, $Z_2 = R_b$ (Fig. 1). σ represent the applied stress.

Resistance and Resistivity

After years of studies and based on the current study on well cements and drilling muds, electrical resistivity (ρ) was selected as the sensing property for both cements and drilling muds. This is unique since in that the same monitoring system can be used to evaluate the performance of cement and drilling muds. Hence, two parameters (resistivity and change in resistivity) will be used to quantify the sensing properties as follows:

$R = \rho (L/A) = \rho K$ ……..……..... (2)

where:
R = electrical resistance
L = Linear distance between the electrical resistance measuring points
A = effective cross sectional area
K = Calibration parameter is determined based on the resistance measurement method

Normalized change in resistivity with the changing conditions can be represented as follows:

$\Delta\rho/\rho = \Delta R/R$ ……..……..... (3)

Resistivity of the materials (ρ) to the changes (composition, curing, stress, fluid loss, and temperature) has been quantified. Correlating the changes, such as composition, curing, stress, cracking, fluid loss, and temperature, to the resistivity (ρ) (Eqn. (2)) and change in resistivity ($\Delta\rho$) (Eqn. (3)) will support the monitoring of the materials (cement and drilling fluid) behavior.

The resistance (R) and capacitance (C) of contacts on the surface are defined as:

$$R = \rho\frac{L}{A} \quad (4)$$

$$C = \epsilon\frac{A}{L} \quad (5)$$

where A = cross-sectional area of contact, L = contact distance (film thickness), ρ = resistivity of the surface film, ϵ = absolute permittivity of the surface film.

The product of equations given in (4) and (5) results as

$$RC = \rho\epsilon \tag{6}$$

Since $\rho\epsilon$ in equation (6) is independent of the film dimension and hence RC is the contact film property. The advantage of Eqn. (6) is that we now are able to characterize the material property of the corrosion products at the interface level as without dependence on the geometry factor such as the length or thickness and area.

Modeling

Curing Model

At least three specimens were tested and the average results about the variation in the resistivity with time up to 1 day and 28 days of curing. Hence the nonlinear model proposed by Vipulanandan and Paul (1990) was modified and used to predict the changes in the electrical resistivity of cement during hydration under different curing conditions and curing time. The proposed Vipulanandan p-q curing model is as follows:

$$\frac{1}{\rho} = \left(\frac{1}{\rho_{min}}\right)\left[\frac{\left(\frac{t+t_o}{t_{min}+t_o}\right)}{q_1+(1-p_1-q_1)*\left(\frac{t+t_o}{t_{min}+t_o}\right)+p_1*\left(\frac{t+t_o}{t_{min}+t_o}\right)^{\frac{q_1+p_1}{p_1}}}\right] \tag{7}$$

Where, ρ is the electrical resistivity (Ω-m); ρ_{min} is the minimum electrical resistivity (Ω-m); t_{min} is the time to reach the minimum electrical resistivity (ρ_{min}). The model parameters were t_o, p_1 (t) and q_1 (t) and t was the curing time (min). The parameter q_1 represents the initial rate of change in the resistivity.

There are three characteristic resistivity parameters that can be used in monitoring the curing (hardening process) of the cement. The resistivity parameters are the initial resistivity (ρ_o), minimum electrical resistivity (ρ_{min}) and time to reach the minimum resistivity (t_{min}).

Stress-Strain Model

Based on the experimental results Vipulanandan p-q Stress-Strain model was used to predict the compressive stress-strain relationship for smart cement with and without NanoFe_2O_3 and the relationship is as follows:

$$\sigma = \left[\frac{\frac{\varepsilon}{\varepsilon_f}}{q_o+(1-p_o-q_o)\frac{\varepsilon}{\varepsilon_f}+p\left(\frac{\varepsilon}{\varepsilon_f}\right)^{\frac{(p_o+q_o)}{p_o}}}\right] * \sigma_f \tag{8}$$

where: σ is compressive stress; σ_f, ε_f are compressive strength and corresponding strain and p_o,q_o are model parameters. Model parameters p_o and q_o increased with curing time based on the NanoFe_2O_3 content.

Piezoresistivity Model

Additional of 0.1% CF substantially improved piezoresistive behavior of the cement. Based on the experimental results, p-q model (Eqn. 16) was modified and used to predict the change in electrical resistivity of cement during with applied stress for 1 day and 28 days of curing. The Vipulanandan p-q piezoresistive model is defined as follows:

$$\frac{\sigma}{\sigma_f} = \left[\frac{\frac{x}{x_f}}{q_2+(1-p_2-q_2)\frac{x}{x_f}+p_2\left(\frac{x}{x_f}\right)^{(p_2/(p_2-q_2))}}\right] \quad \ldots\ldots\ldots\ldots\ldots\ldots \quad (9)$$

where σ compressive stress (MPa); σ_f: stress at failure (MPa); $x = \left(\frac{\Delta\rho}{\rho_o}\right) * 100 =$ Percentage of change in electrical resistivity due to the stress; $x_f = \left(\frac{\Delta\rho}{\rho_o}\right)_f * 100 =$ Percentage of change in electrical resistivity at failure; Δρ: change in electrical resistivity; ρ_o : Initial electrical resistivity (σ=0 MPa) and p_2 and q_2 are piezoresistive model parameters.

4. Materials and Methods

In this study smart cement (Vipulanandan et al. 2014-2016) was used. For the curing and compressive behavior studies cement slurry was cast in plastic cylindrical molds with diameter of 50 mm and a height of 100 mm. Two conductive wires were placed in all of the molds to measure the changing in electrical resistivity. At least three specimens were tested under each condition investigated in this study.

Foam cement Composite

In this study, smart class H cement with water-to-cement of 0.38 was used. The samples were prepared according to the API standards. Commercially available foam was added to the cement slurry and mixed for at least for 5 minutes. After mixing, cement slurries with and without foam were used for fluid loss, curing and piezoresistivity studies.

Iron oxide nanoparticle (NanoFe_2O_3) Composite

Iron oxide nanopowder (NanoFe_2O_3) with the grain size of 30 nm with average specific surface area of 38 m^2/g was used. Also NanoFe_2O_3 was added up to 1% of the smart cement slurry.

Aggregate Composites (Concrete)

Specimens were prepared using smart class H cement with water-cement ratio of 0.38 and adding 10%, 50% and 75% of gravel to the total mix.

Thermal Conductivity

The thermal conductivity of the cement slurries were measured using a commercially available thermal conductivity probe.

Initial resistivity

Two Different methods were used for electrical resistivity measurements of oil well cement slurries. To assure the repeatability of the measurements, the initial resistivity was measured at least three times for each cement slurry and the average resistivity was reported. The electrical resistivity of the cement slurries were measured using:

Conductivity probe

Commercially available conductivity probe was used to measure the conductivity (inverse of resistivity) of the slurries. In the case of cement, this meter was used during the initial curing of the cement. The conductivity measuring range was from 0.1μS/cm to 1000 mS/cm, representing a resistivity of 0.1Ω.m to 10,000 Ω.m.

Digital resistivity meter

Digital resistivity meter (used in the oil industry) was used measure the resistivity of fluids, slurries and semi-solids directly. The resistivity range for this device was 0.01 Ω -m to 400 Ω -m.

The conductivity probe and the digital electrical resistivity device were calibrated using standard solution of sodium chloride (NaCl).

Long-term Resistivity

In this study high frequency AC measurement was adopted to overcome the interfacial problems and minimize the contact resistances. Electrical resistance (R) was measured using LCR meter during the curing time. This device has a least count of 1 μΩ for electrical resistance and measures the impendence (resistance, capacitance and inductance) in the frequency range of 20 Hz to 300 kHz. Based on the impedance (z) – frequency (f) response it was determined that the smart cement was a resistive material (Vipulanandan et al. 2013). Hence the resistance measured at 300 kHz using the two probe method was correlated to the resistivity (measured using the digital resistivity device) to determine the K factor (Eqn.1) for a time period of initial five hours of curing. This K factor was used to determine the resistivity of the cement with the curing time.

Piezoresistivity test

Piezoresistivity describes the change in electrical resistivity of a material under stress. Since oil well cement serves as pressure-bearing part of the oil and gas wells in real applications, the piezoresistivity of smart cement (stress – resistivity relationship) with different w/c ratios were investigated under compressive loading at different curing

times. During the compression test, electrical resistance was measured in the direction of the applied stress. To eliminate the polarization effect, AC resistance measurements were made using a LCR meter at frequency of 300 kHz (Vipulanandan et al. 2013).

Corrosion test

The test setup used in the corrosion measurement is shown below in Figure 6. The test setup includes A1018 Mild Carbon Steel, LCR meter, and two magnetic probes. The interface between the electrical probe and corroding steel contributes to contact resistance and contact capacitance. Bulk steel contributes to the bulk resistance of the circuit.

Flat bar specimens were cut using a dry cutting miter saw to a dimension of 30 inches. At regular intervals measurements were made on the specimens along the length, width and thickness using the LCR device.

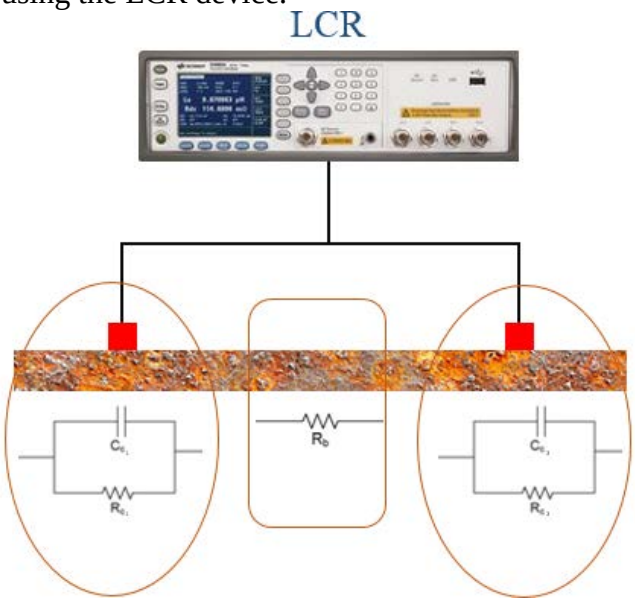

Figure 3. Electrical representation of Nondestructive Electrical testing

5. Results and Discussion

(i) Foam Composite

Thermal Conductivity

The thermal conductivity of the cement slurry with a water-to-cement ratio of 0.38 was 0.802 W/mK. Addition of 5% foam (based on total weight of the cement slurry) reduced the thermal conductivity to 0.482 W/mK, 40% reduction. Increasing the foam content to 20%, reduced the thermal conductivity to 0.284 W/mK, a 65% reduction.

Slurry Piezoresistivity

The impedance – frequency response was similar to additive No. 1 in Fig. 1. The cement slurries with and without foam were subjected to pressure up to 4 MPa in the high pressure high temperature chamber (HPHT) to investigate the piezoresistive behavior.

0% Foam: The resistivity of the smart cement slurry decreased nonlinearly with increase in the pressure (Fig. 4). At 4 MPa pressure the decrease in resistivity was 8%, indicating the piezoresistivity characteristics of the smart cement slurry.

5% Foam: The resistivity of the smart cement slurry with 5% foam decreased nonlinearly with increase in the pressure (Fig. 4). At 4 MPa pressure the decrease in resistivity was 12%, indicating the piezoresistivity characteristics of the smart cement slurry. With 5% foam the piezoresistivity characteristics of the smart foam cement slurry increased by 50%.

20% Foam: The resistivity of the smart cement slurry with 20% foam decreased nonlinearly with increase in the pressure (Fig. 4). At 4 MPa pressure the decrease in resistivity was 22%, indicating the piezoresistivity characteristics of the smart cement slurry. With 20% foam the piezoresistivity characteristics of the smart foam cement slurry increased by 175%, making the smart foam cement to be more sensing.

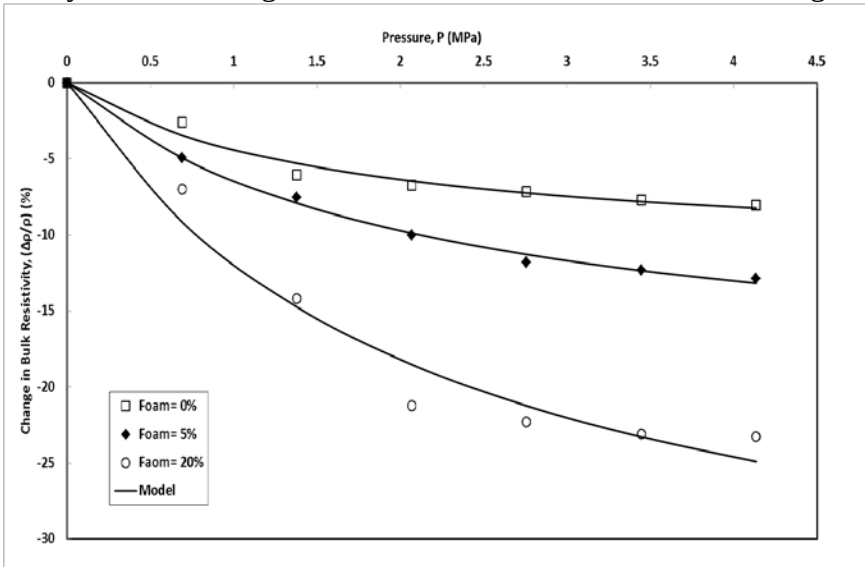

Figure 4. Measured and Predicted Stress-Resistivity Relationship for the Smart Cement With and Without Foam

Fluid Loss

The total fluid loss from the cement slurry at pressure of 0.7 MPa (100 psi) with a water-to-cement ratio of 0.38 was 134 mL (Fig. 6). Addition of 5% foam (based on total weight of the cement slurry) reduced the fluid loss to 31.4 mL, 77% reduction. Increasing the foam content to 20%, reduced the fluid loss to 13.7 mL, a 90% reduction. A hyperbolic model was used to predict the fluid loss with time (Vipulanandan 2014)

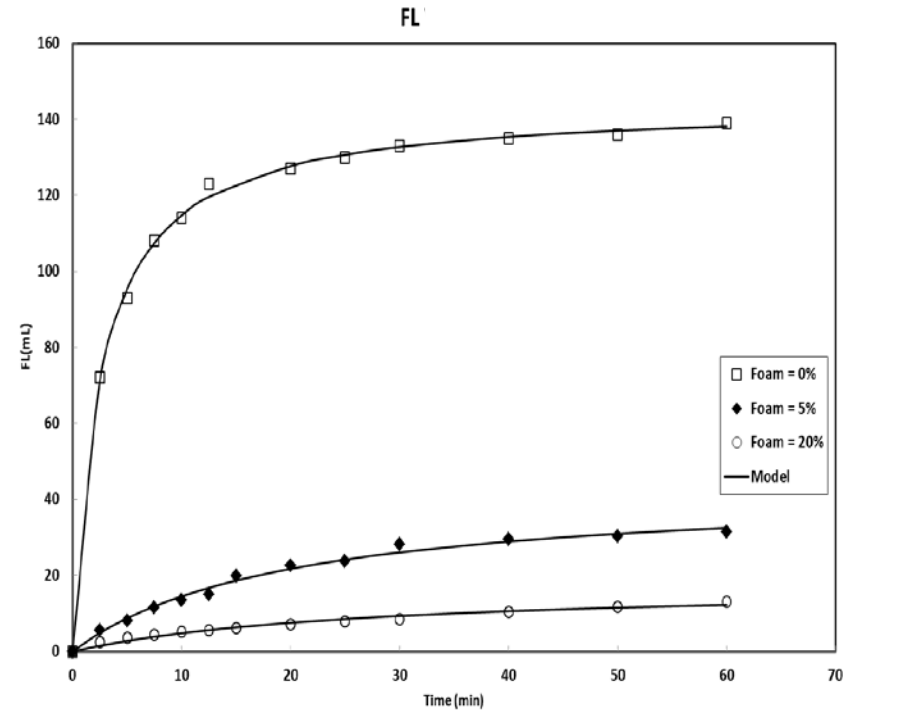

Figure 6 Measured and Predicted Fluid Loss- Time Relationship for the Smart Cement With and Without Foam

The resistivity showed an increasing trend with curing time (Fig. 7) which has been modeled with the curing model (Eqn. (7)). The model parameters were for moisture control curing (zero weight loss): p_1=7.6, q_1=0.6, and t_o=70 min; for room curing: p_1=6.5, q_1=0.82, and t_o=72 min; and for under water curing: p_1=0.83, q_1=0.21, and t_o=58 min.

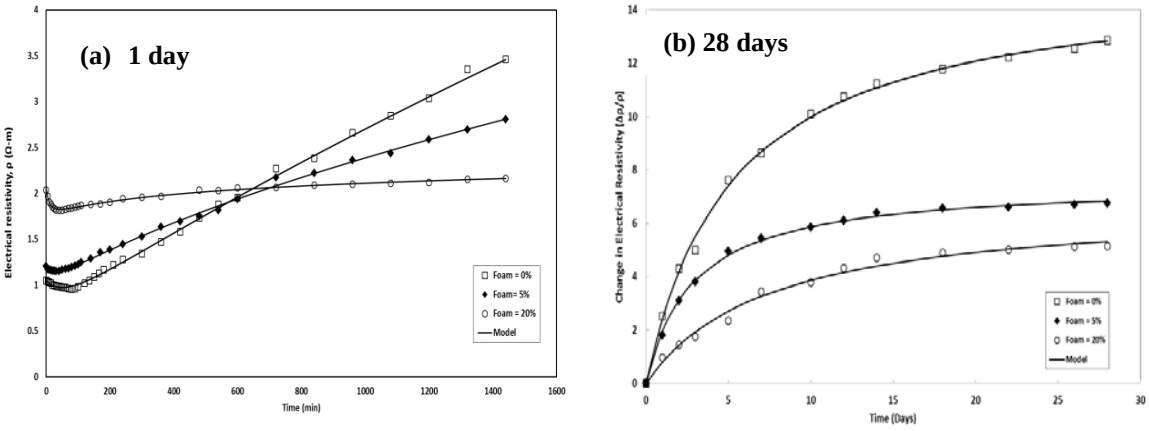

Figure 7 Measured and Predicted Resistivity- Time Relationship for the Smart Cement With and Without Foam (a) One day and (b) 28 days

The resistivity of smart cement with zero foam after 28 days of curing was 14.6 Ω-m, hence the percentage change in resistivity was 1283 %. The resistivity of the 20%

foam cement after 28 days of curing was 12.5 Ω-m, percentage change in resistivity in 28 days was 515% .

Solid Cement Piezoresistivity

0% Foam: The average percentage change in resistance at peak compressive stress of the smart cement after 1 day of curing was 343%. The average percentage change in resistance at peak compressive stress of the smart cement after 28 days of curing was 252%, about 1250 times higher than the compressive strain at failure (0.2%). On an average the piezoresistivity after 28 days of curing was 12.8%/MPa. The model parameter p_2 after 1 and 28 days of curing were 0.1 and 0.001 respectively. The model parameter q_2 after 1 and 28 days of curing were 0.435 and 0.413 respectively.

5% Foam: The average percentage change in resistance at peak compressive stress of the smart cement after 1 day of curing was 304%, a 11% reduction compared to the smart cement without any foam. The average percentage change in resistance at peak compressive stress of the smart cement after 28 days of curing was 188%, about 940 times higher than the compressive strain at failure (0.2%) for smart cement without any foam. On an average the piezoresistivity after 28 days of curing was 12.9%/MPa, comparable to the smart cement without any foam. The model parameter p_2 after 1 and 28 days of curing were 0.083 and 0.001 respectively. The model parameter q_2 after 1 and 28 days of curing were 0.274 and 0.586 respectively.

20% Foam: The average percentage change in resistance at peak compressive stress of the smart cement after 1 day of curing was 113%, a 67% reduction compared to the smart cement without any foam. The average percentage change in resistance at peak compressive stress of the smart cement after 28 days of curing was 98%, about 490 times higher than the compressive strain at failure (0.2%) for smart cement without any foam. On an average the piezoresistivity after 28 days of curing was 18.6%/MPa, higher than the smart cement without any foam. The model parameter p_2 after 1 and 28 days of curing were 0.403 and 0.47 respectively. The model parameter q_2 after 1 and 28 days of curing were 0.605 and 1.07 respectively.

Table 1. Strength, Piezoresistivity and Model Parameters for Smart Cement Foam Composite

					Model Parameters			
	Compressive Strength (MPa)		Peizoresistivity (Δρ/ρ) (%)		P2		q2	
Foam Content	1 Day	28 Days	1 Day	28 Days	1 Day	28 Days	1 Day	28 Days
0	10.29	19.65	343	252.4	0.1	0.001	0.435	0.413
5	4.6	14.6	304	187.9	0.083	0.001	0.274	0.586
20	0.57	5.27	113	98.2	0.403	0.47	0.605	1.07

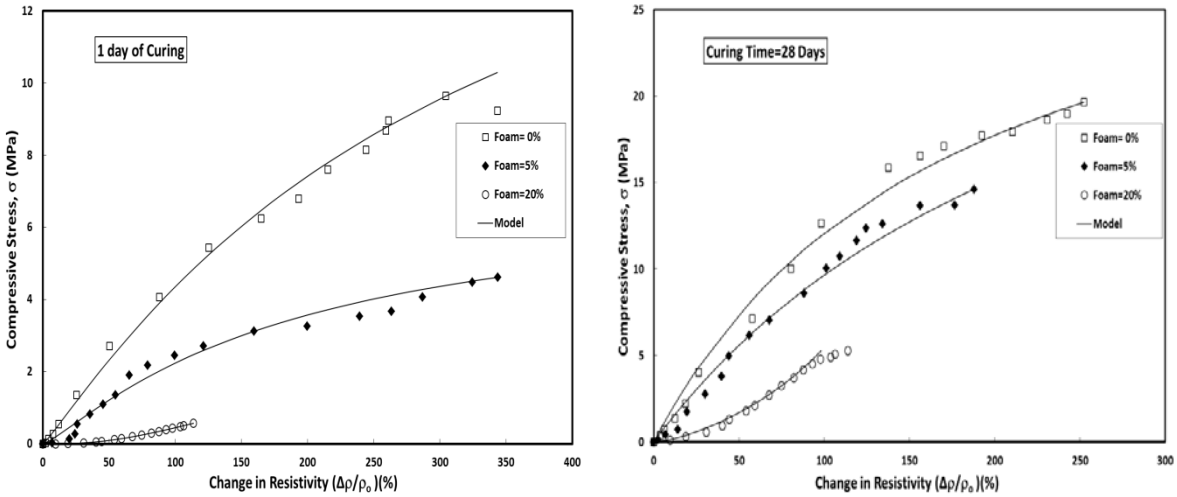

Figure 8. Measured and Predicted Piezoresistivity Relationship for the Smart Cement With and Without Foam and Curing time (a) 1 day and (b) 28 days

(ii) <u>Iron Nanoparticle Composite</u>

The impedance – frequency response was similar to additive No. 2 in Fig. 1. The initial electrical resistivity (ρ_o) of smart cement with 0%, 0.5% and 1% of NanoFe_2O_3 were 1.03 Ω-m, 0.95 Ω-m and 0.87 Ω-m respectively, a 8% and 16% reduction. Also the t_{min} was increased by 7% and 30% when NanoFe_2O_3 concentration increased by 0.5% and 1% respectively. The minimum resistivity (ρ_{min}) of smart cement with 0%, 0.5% and 1% of NanoFe_2O_3 were 0.85 Ω-m, 0.73 Ω-m and 0.66 Ω-m, a 14% and 22% reduction in the electrical resistivity when NanoFe_2O_3 concentration increased by 0.5% and 1% respectively..

Fig. 2 shows the changes in the bulk resistivity of smart cement with different NanoFe_2O_3 content up to 1% after 28 days of curing using the AC measurement.

The model parameter t_o varied between 90 min to 250 min and it decreased with increasing the NanoFe_2O_3 content and curing time. The coefficient of determination (R^2) varied from 0.98 to 0.99 and the root mean square of error (RMSE) varied from 0.02 Ω.m to 0.05 Ω.m based on the NanoFe_2O_3 content and curing time as summarized in Table 3. The t_{min} (min) and ρ_{min} (Ω.m) were correlated with NanoFe_2O_3 content as follows:

$$t_{min} = 27(NanoFe_2O_3(\%)) + 87.5 \qquad R^2=0.91 \quad (10)$$

$$\rho_{min} = 0.85 - 0.2(NanoFe_2O_3(\%)) \qquad R^2=0.98 \quad (11)$$

Hence the NanoFe_2O_3 content linearly correlated to the electrical resistivity parameters.

Compressive Stress-Strain and Piezoresistive Behavior

Compressive Stress-Strain

28 days of curing

The compressive strengths (σ_f) of the smart cements with 0%, 0.5%, and 1% $NanoFe_2O_3$ after 28 days of curing were 19.3 MPa, 25.4 MPa and 27 MPa, respectively a 32% and 40% increase due to the addition of 0.5% and 1% $NanoFe_2O_3$, respectively, as shown in Fig. ?. Additional of 1% $NanoFe_2O_3$ increased the initial modulus of elasticity after 28 days of curing from 1936 MPa to 2479 MPa, a 28% increase. The axial strain of the samples at failure varied between 0.2% to 0.28%. The model parameters q_o and p_o increased with curing time and $NanoFe_2O_3$ content. The coefficients of determination (R^2) was 0.99.

Piezoresistivity

28 days of curing

Addition of 0.1% CF to the cement enhanced the change in electrical resistivity of the smart cement at failure $\left(\frac{\Delta\rho}{\rho_o}\right)_f$ by a factor of 520. Addition of 0.5% and 1% of $NanoFe_2O_3$ further increased the change in electrical resistivity of smart cement at failure $\left(\frac{\Delta\rho}{\rho_o}\right)_f$ by 53% and 60% respectively as summarized in Table 5. The model parameter q_2 and p_2 are summarized in Table 5. The coefficients of determination (R^2) were 0.99. The root mean square of error (RMSE) varied between 0.012 MPa and 0.02 MPa.

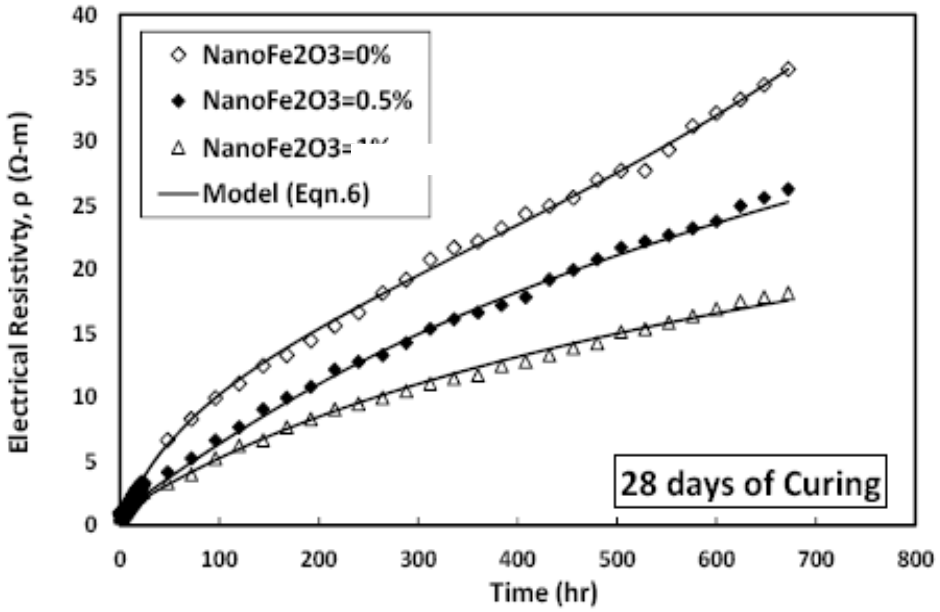

Figure 10. Variation of Resisvity with Curing time and NanoFe content

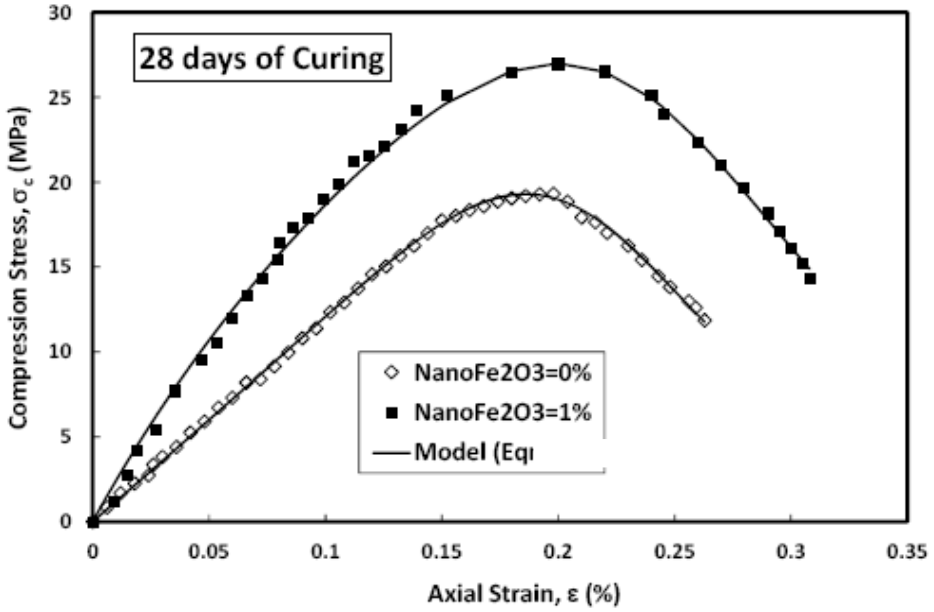

Figure 11. Compressive Stress-Strain Relationship For Smart Cement with 1% NanoFe content

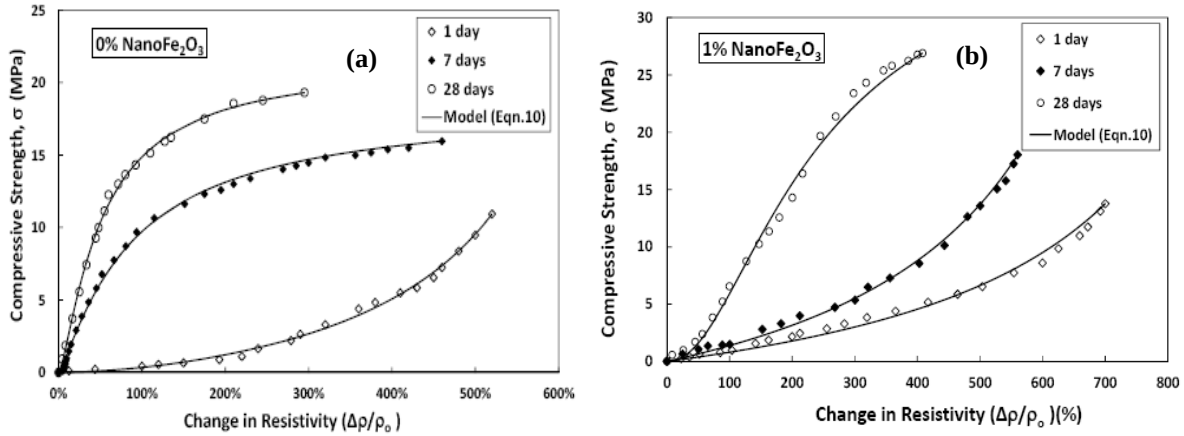

Figure 12. Measured and Predicted Piezoresistivity Relationship for the Smart Cement With and Without Foam and Curing time (a) 1 day and (b) 28 days

(iii) *Aggregate Composites (Concrete)*

The impedance – frequency response was similar to additive No. 1 in Fig. 13. The compressive strength of the cement was 1.24 ksi after1 day of curing. Adding 10%, 50% and 75% of gravel to smart cement increased the compressive strength by 12%, 28% and 32% to 1.39 ksi, 1.59 ksi and 1.64 ksi respectively. As shown in Fig.13, after 1 day of curing, the piezoresistivity of the smart cement was 375%. Parameters *p* and *q* for the model were 0.68 and 0.61 respectively. The ultimate piezoresistivity of smart concrete with 10%, 50% and 75% of gravel were decreased by 6%, 23% and 42% respectively to

354%, 288% and 217%. The model parameters p_2 and q_2 are summarized in Table 2.

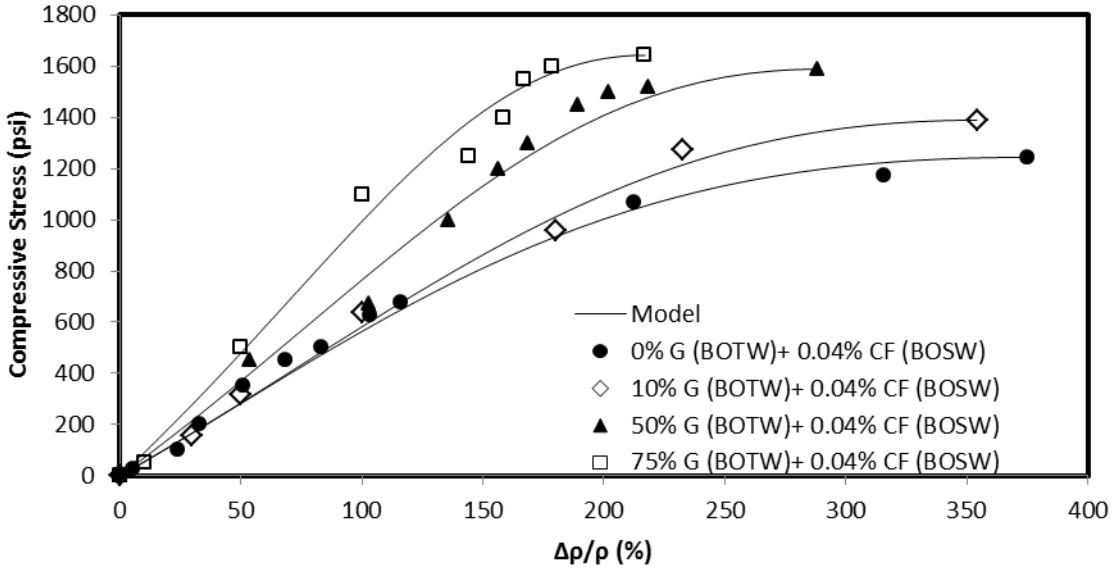

Figure 13. Piezoresistive behavior of the smart concrete after 1 day of curing

Table 2. Model parameters of p-q model for evaluating the piezoresistive behavior, Compressive Strength and Ultimate Piezoresistivity of the smart concrete after 1 day of curing

Cement	1 Day Curing			Compressive Strength (psi)	Ultimate Piezoresistivity (%)
	$p_{2\ Day}$	$q_{2\ Day}$	R^2		
Smart Cement	0.68	0.61	0.99	1240	375
10% Gravel Smart Concrete	0.55	0.72	0.99	1390	354
50% Gravel Smart Concrete	0.51	0.79	0.99	1590	288
75% Gravel Smart Concrete	0.44	0.85	0.99	1640	217

Corrosion Study

The impedance – frequency response was similar to additive No. 2 in Fig. 1. Upon 500 days of corrosion of steel in 3.5% NaCl solution, R_b had changed by about 50,000 times which proves the corrosion process taking place in the electrochemical system.

For the 8 inches distance measurement, bulk resistance increased from 0.111 Ω to 4613 Ω with 500 days of corrosion, which shows a tremendous change of 41558 times, similarly for 16 inches distance measurement, bulk resistance increased from 0.124 Ω to 5042 Ω, which shows a change of 40661 times and finally for 24 inches distance measurement, bulk resistance increased from 0.131 Ω to 5810 Ω, which showed a change of 44,351 times. All these changes indicate that inner layer of steel is also corroding which would not be reported in using other corrosion testing methods.

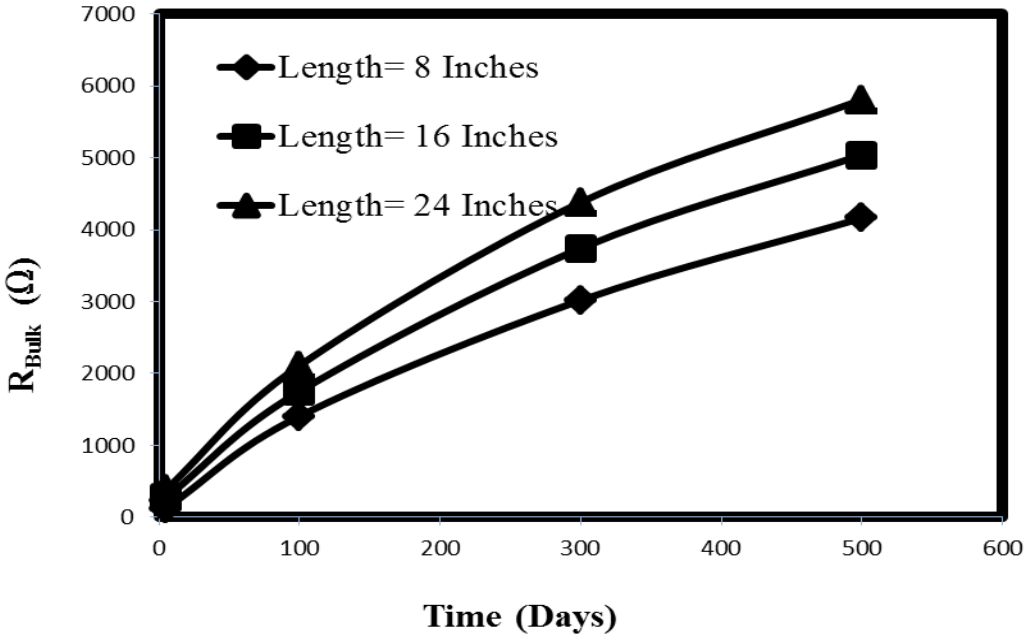

Figure 14. Bulk Resistance with Time (500 Days)

.

Bulk Resistivity

The resistivity of the material was calculated using the Eqn. (1). The resistivity of the steel increased from 1.59 x10^{-7} Ωm to 5.96 x10^{-3} Ωm for length of 8 inches, 1.59 x10^{-7} Ωm to 6.47 x10^{-3} Ωm for length of 16 inches and 1.59 x10^{-7} Ωm to 7.05 x10^{-3} Ωm for length of 24 inches in a testing period of 500 days, which indicated the corrosion level was high. These values also indicate that the metal is turning from conductive to the insulative material.

This corrosion relationship indicated that the rate of corrosion decreasing with time but still corrosion process was continuing. As rust is an oxide compound, with an increase in corrosion or rust formation, the resistance and resistivity of the material start to increase, by which we obtain this result. As the corrosive ions are getting depleted, we could see the drop in corrosion rate as time increases. Hence this proves the accuracy of the corrosion measurement.

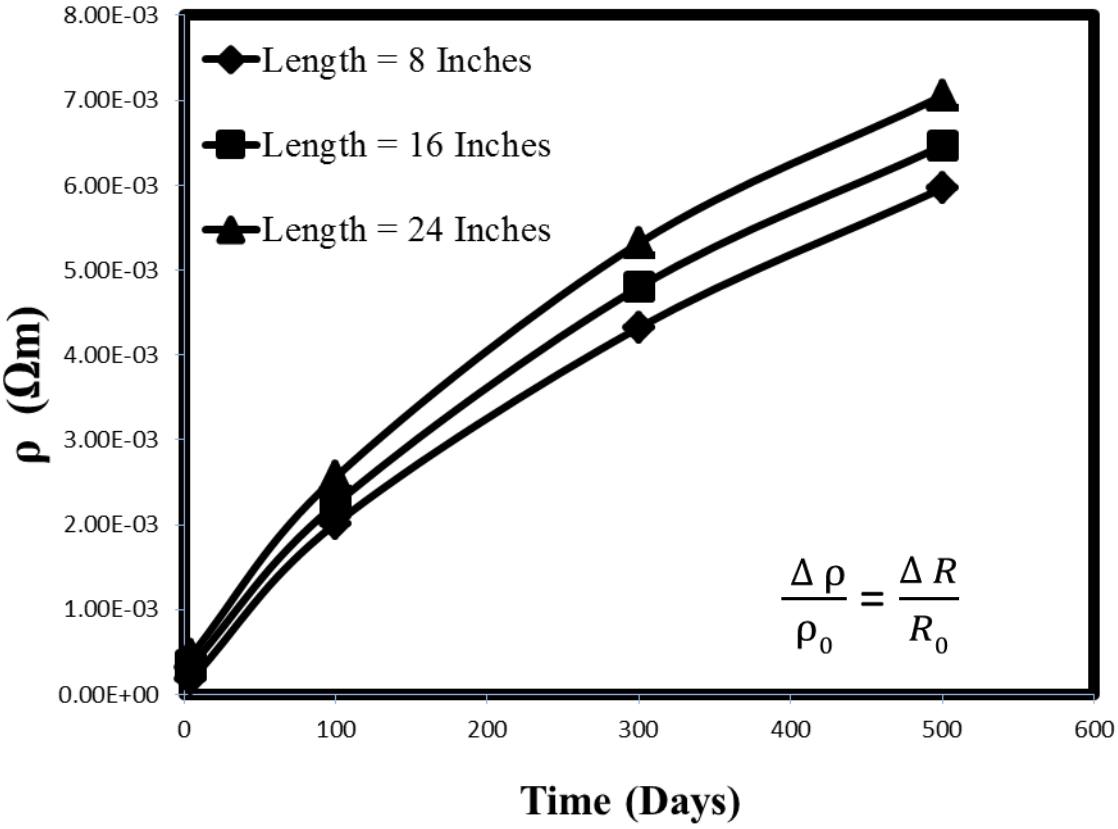

Figure 15. Electrical Resistivity of the Steel Specimen with Time (500 Days) in 3.5% Salt Solution.

Surface Characterization

The higher RcCc value of the one contact point indicated that the steel specimen was corroding. The R_CC_C value of the steel specimen increased from 1.51 E-06 ΩF to 1.82 E-05 ΩF during the testing period of 500 days, which indicated that the steel was corroding. In 500 days the surface corrosion parameter increased by 1,110%.

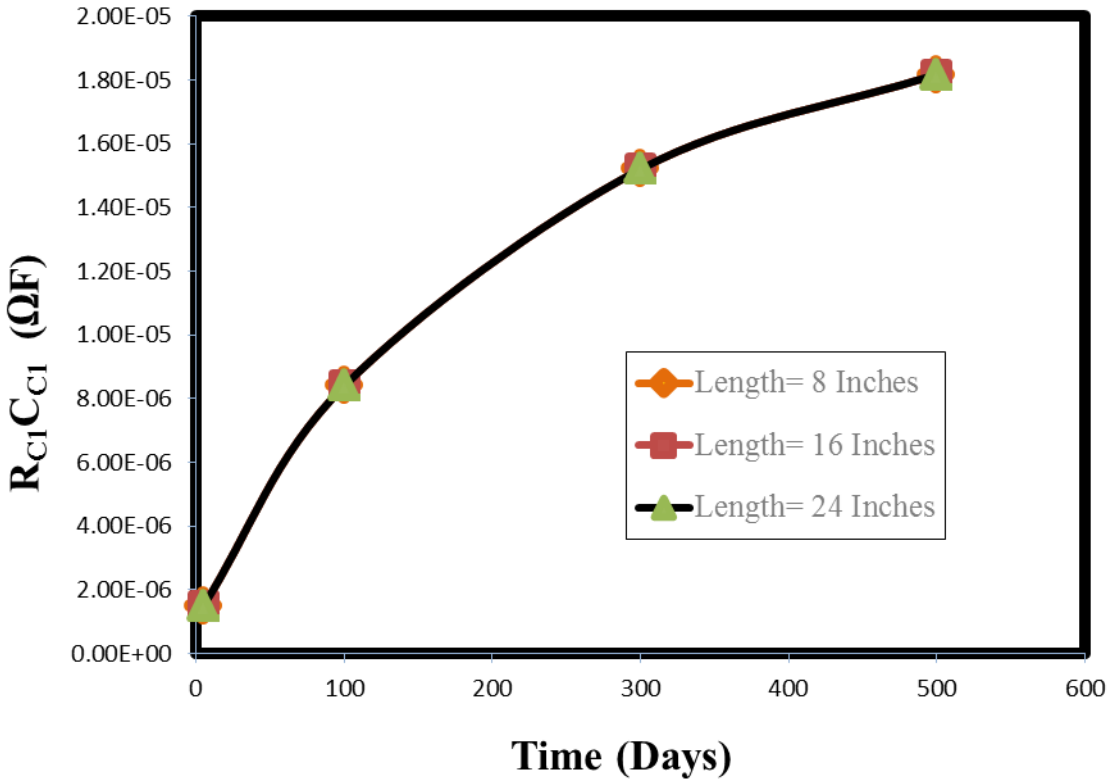

Figure 16. Material Property R_cC_c of Contact 1 of the corroding steel specimen in 3.5 % NaCl Solution

The pulse velocity in the steel is directly proportional to its elastic modulus and density. The corrosion of the steel affected the pulse velocity. Un-corroded steel during the first month had a velocity was 6220 m/s for 24 Inches distance measurement. Corroded steel after the third month had a velocity of 3908 m/s for 24 inches distance measurement. Steel after one year of corrosion had a velocity of 2498 m/s for the 24 inches distance measurement. It was observed that with corrosion the pulse velocity decreased with time.

It was well proved that nondestructive electrical method using resistivity outperformed standard weight loss method which showed a 0.27 % change in 1 year, pulse velocity method showed 63 % change in 1 year and nondestructive electrical method showed a change in the bulk resistivity of 4,876,363 %.

6. Conclusions

Based on the smart cement composite and corrosion study following conclusions are advanced.

(1) The two-probe method was effective in measuring the bulk resistance of the smart cement composites and the corroding steel. This approach of using the two probe with LCR meter can be used for real-time monitoring of the changes.

(2) Smart foam cement slurry was piezoresistive and the resistivity change increased with the foam content. With the addition of 20% foam, the resistivity change at 4 MPa (600 psi) increased from 8% for the smart cement slurry with no foam to 22% with 20% foam, about 175% increase in the piezoresistivity.

(3) The total fluid loss for the smart cement at 0.7 MPa (100 psi) pressure was reduced from 134 mL to 13 mL with the addition of 20% foam, about a 90% reduction.

(4) Addition of 20% foam (by weight) increased the initial electrical resistivity of smart cement from 1.05 Ωm to 2.04 Ωm, a 93% increase. Addition of foam affected the curing of the cement based on the resistivity measurements. The average compressive strength of the smart foam cement after 1 day of curing was 0.57 MPa, about 94% reduction in strength compared smart cement without any foam. The average compressive strength of the smart foam cement after 28 days of curing was 5.27 MPa, a 825% increase in strength. The 28^{th} day compressive strength of smart foam cement was 73% less than compressive strength of the smart cement without any foam.

(5) The solidified smart cement with and without foam were piezoresistive. The average percentage change in resistance at peak compressive stress of the smart foam cement with 20% foam after 1 day of curing was 113%, a 67% reduction compared to the smart cement without any foam. The average percentage change in resistance at peak compressive stress of the smart foam cement after 28 days of curing was 98%, about 490 times higher than the compressive strain at failure (0.2%) for smart cement without any foam. On an average the piezoresistivity after 28 days of curing was 18.6%/MPa, higher than the smart cement without any foam.

(6) Initial resistivity was sensitive to the amount of NanoFe_2O_3 used to modify the smart cement. The amount of NanoFe_2O_3 can be detected based on the change in the initial resistivity. Addition of 1% NanoFe_2O_3 decreased the initial electrical resistivity (ρ_o) of smart cement by 16% and reduced the time to reach minimum resistivity (t_{min}) by 27 minutes. Initial electrical resistivity can be used as a good indicator for quality control. The nonlinear curing model quantified the curing of the smart cement with and without NanoFe_2O_3.

(7) Addition of NanoFe_2O_3 further enhanced the piezoresistivity behavior of the smart cement. The piezoresistivity of smart cement with NanoFe_2O_3 was over 750 times higher than the unmodified cement depending on the curing time and nanoparticles content. The nonlinear piezoresistivity model predicted the compressive piezoresistivity of the smart cement very well with and without NanoFe_2O_3.

(8) Addition of 1% NanoFe_2O_3 increased the compressive strength of the smart cement by 26% and 40% after 1 day and 28 days of curing respectively. The modulus of elasticity of the smart cement increased with additional of 1% NanoFe_2O_3 by 29% and 28% after 1 day and 28 days of curing respectively.

(9) Addition of aggregates also showed that the smart cement aggregate (concrete) was piezoresisitive. With the addition of aggregate the piezoresistivity of the composite decreased.

(10) The Vipulanandan p-q curing, stress-strain and piezoresistive models predicted the experimental trends very well for all the smart cement composites.

(11) Steel specimen exposed to 3.5% NaCl solution for a period of 500 days showed that the resistivity of the steel specimen increased from 1.59 $x10^{-7}$ Ωm to 5.96 $x10^{-3}$ Ωm for measurement length of 8 inches, 1.59 x10-7 Ωm to 6.47 x10-3 Ωm for measurement length of 16 inches and 1.59 $x10^{-7}$ Ωm to 7.05 $x10^{-3}$ Ωm for measurement length of 24 inches in a testing period of 500 days.

(12) The surface of the steel corroded and a new thin film surface electrical parameter R_cC_c increased due to corrosion of the steel. The surface corrosion parameter R_cC_c of the steel specimen increased from 1.51 E-06 ΩF to 1.82 E-05 ΩF.

7. Acknowledgements

This study was supported by the Center for Innovative Grouting Materials and Technology (CIGMAT) and the Texas Hurricane Center for Innovative Technology (THC-IT) at the University of Houston, Texas with funding from DOE/NETL/RPSEA (Project No. 10121-4501-01) and industry. Sponsors are not responsible for all the conclusion made from this study.

8. References

1. API Recommended Practice 10B (1997), Recommended Practice for Testing Well Cements Exploration and Production Department, 22nd Edition.
2. API Recommended Practice 65 (2002), Cementing Shallow Water Flow Zones in Deepwater Wells.
3. Carter, K. M. and Oort, E. (2014), Improved Regulatory Oversight Using Real-Time Data Monitoring Technologies in the Wake of Macondo, SPE 170323, pp. 1-51.
4. Izon, D. and M. Mayes, M. (2007), "Absence of fatalities in blowouts encouraging in MMS study of OCS incidents 1992-2006," Well Control Magazine, pp. 86-90.
5. John B., (1992). "Class G and H Basic Oil Well Cements," World Cement.
6. Kyle, M. and Van Eric (2014), Improved regulatory oversight using real- time data monitoring technologies in the Wake of Macondo, SPE 170323, pp. 1-51.
7. Vipulanandan, C. and Paul, E. (1990) "Performance of epoxy and polyester polymer concrete," ACI Materials Journal, Vol. 87, No. 3, pp. 241–251.

8. Vipulanandan, C., and Sett, K. (2004), "Development and Characterization of Piezoresistive Smart Structural Materials", Proceedings, Engineering, Construction and Operations in Challenging Environments, Earth & Space 2004, ASCE Aerospace Division, League City, TX, pp. 656-663.
9. Vipulanandan, C., and Liu, J. (2005), "Polyurethane Based Grouts for Deep Off-Shore Pipe-in-Pipe Application", Proceedings, Pipelines 2005, ASCE, Houston, TX, pp. 216-227.
10. Vipulanandan, C., and Garas, V. (2006), "Piezoresistivity of Carbon Fiber Reinforced Cement Mortar", Proceedings, Engineering, Construction and Operations in Challenging Environments, Earth & Space 2006, Proceedings ASCE Aerospace Division, League City, TX, CD-ROM.
11. Vipulanandan, C., Dimrican, E., and Harendra, S. (2010), "Artificial Neural Network and Nonlinear Models for Gelling and Maximum Curing Temperature Rise in Polymer Grouts," Journal of Materials in Civil Engineering, Volume 23, No. 4, p. 1-6.
12. Vipulanandan, C. and Prasanth, P., (2013)" Impedance Spectroscopy Characterization of a piezoresistive Structural Polymer Composite Bulk Sensor," Journal of Testing and Evaluation, Vol. 41, No.6, 898-904.
13. Vipulanandan et al. (2014a), "Development and Characterization of Smart Cement for Real Time Monitoring of Ultra-Deepwater Oil Well Cementing Applications, OTC-25099-MS.
14. Vipulanandan et al. (2014b), "Characterization of Smart Cement Modified with Sodium Meta Silicate for Ultra-Deepwater Oil Well Cementing Applications, AADE-2014.
15. Vipulanandan, C. Heidari, M., Qu, Q., Farzam, H., and Pappas, J. M. (2014c), "Behaviour of piezoresistive smart cement contaminated with oil based drilling mud," Offshore Technology Conference, OTC 25200-MS, pp. 1-14.
16. Vipulanandan, C. and Mohammed, A. (2014d), "Hyperbolic rheological model with shear stress limit for acrylamide polymer modified bentonite drilling muds," Journal of Petroleum Science and Engineering, 122, 38–47.
17. Vipulanandan, C., and Mohammed, A., (2015a) "Smart cement rheological and piezoresistive behavior for oil well applications." Journal of Petroleum Science and Engineering, V-135, 2015, pp. 50-58.
18. Vipulanandan, C., and Mohammed, A., (2015b) "Smart cement modified with iron oxide nanoparticles to enhance the piezoresistive behavior and compressive strength for oil well applications." Journal of Smart Materials and Structures, Vol. 24 Number 12, pp. 1-11.
19. Vipulanandan, C, Krishnamoorti, R. Mohammed, A., G. Narvaez, Head, B. and Pappas, J. (2015c) "Iron Nanoparticle Modified Smart Cement for Real Time Monitoring of Ultra Deepwater Oil Well Cementing Applications", Offshore Technology Conference (OTC) 2015, OTC-25842-MS, pp. 1-20..
20. Vipulanandan, C, Ramanathan, P. Ali, M., Basirat, B. and Pappas, J. (2015d) "Real Time Monitoring of Oil Based Mud, Spacer Fluid and Piezoresistive Smart Cement to Verify the Oil Well Drilling and Cementing Operation Using Model Tests", Offshore Technology Conference (OTC) 2015, OTC-25851-MS, pp. 1-18.

21. Vipulanandan, C. and Ali, K. (2016) "Smart Cement Piezoresistive Behavior with and without Sodium Meta-silicate Under Temperature and Curing Environments for Oil Well Applications," Journal of Civil Engineering Materials, American Society of Civil Engineers (ASCE), doi 10.1061/MT.1943-055330001667

22. Zhang, M., Sisomphon, K., Ng, T.S, and Sun, D.J, (2010a). "Effect of superplasticizers on workability retention and initial setting time of cement pastes," Construction and Building Materials 24, 1700–1707.
23. Zhang, J., Weissinger, E.A, Peethamparan, S, and Scherer, G.W., (2010b). "Early hydration and setting of oil well cement," Cement and Concrete research, Vol. 40, 1023-1033.